Journal of Biomolecular NMR, 4 (1994) 215–230
ESCOM

J-Bio NMR 172

Analysis of proton chemical shifts in regular secondary structure of proteins

Klara Ösapay and David A. Case

Department of Molecular Biology, The Scripps Research Institute, La Jolla, CA 92037, U.S.A.

Received 24 August 1993
Accepted 30 September 1993

Keywords: Chemical shift; Secondary structure

SUMMARY

The contribution of peptide groups to H^{α} and H^{β} proton chemical shifts can be modeled with empirical equations that represent magnetic anisotropy and electrostatic interactions [Ösapay, K. and Case, D.A. (1991) *J. Am. Chem. Soc.*, **113**, 9436–9444]. Using these, a model for the 'random coil' reference state can be generated by averaging a dipeptide over energetically allowed regions of torsion-angle space. Such calculations support the notion that the empirical constant used in earlier studies arises from neighboring peptide contributions in the reference state, and suggest that special values be used for glycine and proline residues, which differ significantly from other residues in their allowed ϕ,ψ-ranges. New constants for these residues are reported that provide significant improvements in predicted backbone shifts. To illustrate how secondary structure affects backbone chemical shifts we report calculations on oligopeptide models for helices, sheets and turns. In addition to suggesting a physical mechanism for the widely recognized average difference between α and β secondary structures, these models suggest several additional regularities that should be expected: (a) H^{α} protons at the edges of β-sheets will have a two-residue periodicity; (b) the $H^{\alpha 2}$ and $H^{\alpha 3}$ protons of glycine residues will exhibit different shifts, particularly in sheets; (c) H^{β} protons will also be sensitive to local secondary structure, but in different directions and to a smaller extent than H^{α} protons; (d) H^{α} protons in turns will generally be shifted upfield, except those in position 3 of type I turns. Examples of observed shift patterns in several proteins illustrate the application of these ideas.

INTRODUCTION

The existence of close connections between chemical shifts and local secondary structure in proteins has been well known for some time (Dalgarno et al., 1983; Pardi et al., 1983; Szilágyi and Jardetzky, 1989; Pastore and Saudek, 1990; Wishart et al., 1991), and the growing number of NMR assignments of proteins has made possible analyses with increased statistical significance. For protons, considerable attention has been paid to ways in which the H^{α} shifts reflect local secondary structure. It has been recognized for some time that β- or extended regions show downfield shifts for this resonance, while helical regions show upfield shifts (Dalgarno et al.,

0925-2738/$ 10.00 © 1994 ESCOM Science Publishers B.V.

1983; Szilágyi and Jardetzky, 1989; Pastore and Saudek, 1990; Williamson, 1990; Wishart et al., 1991). The most extensive survey is that of Wishart et al. (1991), who considered shifts in over 70 proteins with assigned secondary structures. In this study, the mean H^{α} shifts in helices and sheets differed by nearly 0.8 ppm and there was remarkably little overlap between the two distributions. These relations, and others seen for amide protons and ^{13}C and ^{15}N shifts (Kuntz et al., 1991; Spera and Bax, 1991; Wishart et al., 1991; De Dios et al., 1993), are in many cases clear enough to drive secondary structure assignments (Andersen et al., 1992; Wishart et al., 1992), but do not identify the physical interactions responsible for the correlations seen, and do not allow easy extrapolation to other situations.

In both organic chemistry and biochemistry, empirical analyses of the effects of 'distant' substituents on chemical shifts have played an important interpretive role for many years (Harris, 1986). There are generally two such types of interactions in liquids: local magnetic fields arising from anisotropies in the magnetic susceptibilities of distant functional groups, and local electric fields created by distant dipoles or charges. The former are strongest for conjugated or partially delocalized electrons (as in aromatic rings or peptide groups) and simply augment or oppose the external magnetic field (McConnell, 1957; Haigh and Mallion, 1980). Electrostatic fields influence chemical shifts indirectly, by polarizing chemical bonds, and thus contribute to shielding or deshielding of the nuclei (Buckingham, 1960). Electric-field effects can be difficult to estimate for proteins in water, because solvent polarization contributions are quite important (Sharp and Honig, 1990; Warshel and Aqvist, 1991), but recent empirical analyses suggest that both electric-field and magnetic anisotropy effects contribute in significant ways to proton chemical shifts in proteins (Ösapay and Case, 1991; Williamson and Asakura, 1993).

In folded proteins, the conformation-dependent part of the chemical shift can be defined as the difference between the observed shift and the 'random coil' value (Bundi and Wüthrich, 1979) of the same type of proton and amino acid. These 'structural' shifts can be approximated by calculating contributions of ring currents of aromatic groups, magnetic anisotropy contributions from peptide groups, and electrostatic effects arising from charges and dipoles. Different models that have been calibrated against experimental data result in fairly good predictions for α-protons (Williamson and Asakura, 1991,1993; Williamson et al., 1992) and for all carbon-attached protons (Ösapay and Case, 1991). For example, our previous model (Ösapay and Case, 1991) uses a simple summation of the above contributions:

$$\Delta\delta \equiv \delta^{obs}_{prot} - \delta^{obs}_{random\ coil} \approx \sum \delta_{rc} + \sum \delta_{m} + \sum \delta_{el} - \delta_{const} \qquad (1)$$

Here rc, m and el refer to ring current, peptide-group anisotropy, and electrostatic interactions, respectively. The δ_{const} parameter was originally treated as a fitting parameter, but is likely to reflect (at least in part) the contributions from δ_m and δ_{el} that are present even in the random-coil reference state. Here we test this interpretation through calculations on dipeptide models, averaging $\delta_m + \delta_{el}$ over a distribution of conformers that mimics that of an unconstrained peptide. The results support the original interpretation, and suggest the introduction of new constants for glycine and proline residues, whose intrinsic ϕ–ψ distributions are different from those for other amino acids. In addition, we explore the expected behavior of backbone proton shifts in models of regular secondary structure, pointing out a variety of expected regularities in shift behavior that go beyond the trends mentioned above.

METHODS

Peptide modeling

The program CHARMm (Brooks et al., 1983) was used to generate peptide models with standard geometric parameters given in the CHARMm22 parameter set. For the alanine, glycine and proline dipeptides, the ϕ and ψ torsional angles were varied at 10° increments, and all remaining degrees of freedom minimized to produce an 'adiabatic' ϕ–ψ map. These gas-phase energies do not reflect important solvation contributions that are known to change the relative energies of dipeptide configurations, in particular by stabilizing α-configurations ($\phi < 0$, $\psi < 0$) relative to more extended forms (Anderson and Hermans, 1988; Pettitt and Karplus, 1988; Brooks and Case, 1993). We have estimated these solvation terms using a continuum dielectric model for the solvent, combined with numerical solutions of the Poisson–Boltzmann equation using the MEAD (Macroscopic Electrostatics with Atomic Detail) set of programs (Bashford and Karplus, 1990; Bashford and Gerwert, 1992). Here the solvation free energy is taken as the difference in electrostatic energy required to charge the solute for continuum 'solvents' with $\varepsilon = 80$ and $\varepsilon = 1$. The peptide charges used are those from the CHARMm22 empirical potential (Brooks et al., 1983) and the solute cavity is taken as the solvent-accessible molecular surface, defined using atomic (or 'Born') radii as suggested by Bondi (Bondi, 1964), and shown to give a good account of electrostatic contributions to solvation in various circumstances (Bashford et al., 1993; Honig et al., 1993). A more detailed description of the method is given elsewhere (Bashford and Gerwert, 1992), and the results for relative solvation energies of the alanine dipeptide conformers have been shown to be in good agreement with estimates from free energy simulations that use a more microscopic description of the solvent contribution (Brooks and Case, 1993). This technique includes only the electrostatic contribution to solvation free energies, but this is likely to dominate free energy differences for this system (Grant et al., 1990); for example, the solvent-accessible molecular surface area for the alanine dipeptide varies by only about 15 Å^2 over the entire ϕ–ψ range, so that cavity and dispersion terms (which are approximately proportional to surface area) should vary only by a small amount as a function of conformation.

Models for regular secondary structure were constructed as follows. A 21-residue polyalanine with $\phi = -65$ and $\psi = -40$ was generated as a model for an α-helix. Two extended chains of 10-residue polyalanine molecules with $\phi = -120$ and $\psi = 120$ served as a model for β-structures. The precise choice of angles is somewhat arbitrary, but these serve to create 3D models in the appropriate regions of (ϕ, ψ) space. The β-strands were visually docked into parallel or antiparallel sheets, and the relative orientation minimized using the CHARMm19 parameter set. Models of the four most frequently occurring turns were generated using the idealized torsion angles given in Table 1. Turns VIa and VIb contain a *cis*-proline at position three. Ball-and-stick figures for all of these structures are given below.

Chemical shift calculations

The sum of the electrostatic and peptide-group anisotropy contributions to structural shifts was calculated using our earlier model (Ösapay and Case, 1991), as implemented in the SHIFTS program (Cross and Wright, 1985; Ösapay et al., 1991). This program is available by anonymous ftp from riscsm.scripps.edu, file pub/shifts.tar.Z. SHIFTS requires an input file in Brookhaven

(PDB) format; functionally equivalent code is also available as part of the AMBER molecular modeling package (Pearlman et al., 1991).

The use of a dipeptide model for the 'random coil' state implicitly assumes that the most important contributions to backbone proton chemical shifts arise from the neighboring peptide groups, and this assumption is examined below. Acetylalanine-*N*-methylamide and its glycine and proline analogues (the 'dipeptides') were used for investigating the contributions of the two peptide groups to the chemical shifts for the α- and β-protons of the central amino acid when φ and ψ are varied. The distribution of conformers was described by a Boltzmann distribution, using the energies estimated as described above. Hence the average shift in the 'unstructured' dipeptide is

$$\delta = \frac{\int\int (\delta_m + \delta_{el}) \exp[-E(\phi, \psi)/kT]\, d\phi d\psi}{\int\int \exp[-E(\phi, \psi)/kT]\, d\phi d\psi} \quad (2)$$

We have approximated the integration by a summation in 10° increments; k is the Boltzmann constant and T = 308 K.

RESULTS

Dependence on φ- and ψ-angles

H^α shifts. Figure 1A shows a 3D plot of the structural chemical shifts of the α-proton vs. two torsional angles in the dipeptide model. As we noted before (Ösapay and Case, 1991), the dependence on ψ is only a weak one, so that the principal structural variation arises from φ. (For proline, the electrostatic contribution is slightly different from that for other residues, because of the difference in atomic partial charges, but the results are practically the same.) The difference in chemical shifts between helical and extended conformations is about 0.6 ppm: the calculated structural shift in the helical region, where φ is about −65° and ψ is about −40°, is −0.14 ppm, and in the β-region, where φ is about −120° and ψ is about 120° the α-proton chemical shifts are around +0.45 ppm. Analyses of the general level of agreement of such estimates with observed shifts in proteins have been presented earlier (Ösapay and Case, 1991; Williamson and Asakura, 1993). A somewhat different, and flatter, dependence on φ and ψ has been calculated by Asakura et al. (1992); we do not understand the origins of this difference, but the overall agreement with experimental H^α shifts is better with the formula used in Fig. 1A.

H^β shifts. We have also investigated the effect of the backbone conformation on the protons

TABLE 1
TORSIONAL ANGLES IN 4-RESIDUE PEPTIDE MODELS

	ϕ_2	ψ_2	ϕ_3	ψ_3
Type I	−60	−30	−90	0
Type II	−60	120	80	0
Type VIa	−60	140	−80	0
Type VIb	−140	120	−60	140
α	−65	−40	−65	−40
β	−120	120	−120	120

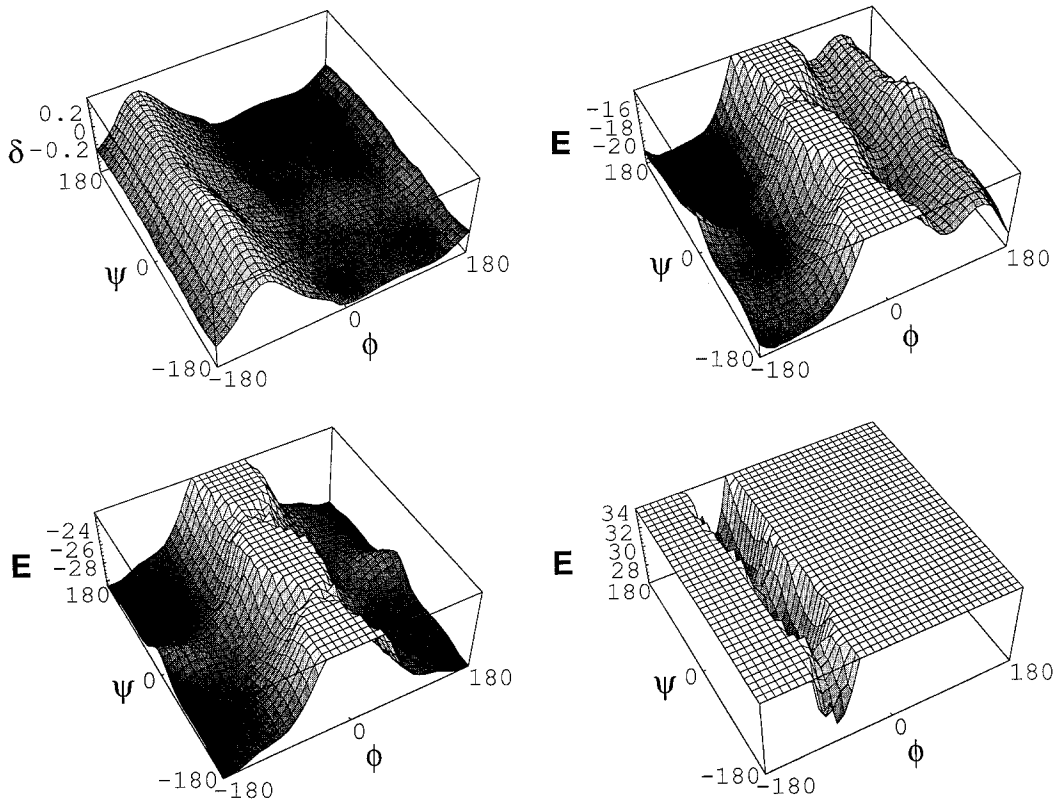

Fig. 1. (A) Calculated structural shifts for the α-proton in a dipeptide as a function of the ϕ and ψ dihedral angles. Ramachandran plots calculated by the CHARMm22 potential and corrected by the MEAD solvent for (B) alanine dipeptide; (C) glycine dipeptide; and (D) proline dipeptide.

attached to C^{β}. In alanine, where the shifts of the methyl protons are averaged, the variation with ϕ and ψ is less than 0.3 ppm in the whole 'allowed' region, and values in the helical region are only 0.05 ppm larger than shifts in the β-regions. For stereoassigned β-methylene protons, the difference between helical and β-sheet conformations is about 0.1 ppm for $H^{\beta 2}$, if we assume a rigid side-chain conformation with $\chi^1 = 180°$ (i.e., the α-helical shift is slightly downfield from the value in β-structures). For $H^{\beta 3}$, the difference is half as much, in the opposite direction. The average shift of the two β-methylene protons is 0.04 ppm downfield in α-helices with respect to the shifts in extended chains. All of these values suggest that H^{β} shifts should be much less useful than the backbone shifts in offering qualitative indicators of local secondary structure, and that the small empirical value of δ_{const} found earlier (0.04 ppm, Ösapay and Case, 1991) is appropriate.

Averaged shifts in unstructured peptides

When we use Eq. 2 to calculate the shift in the 'random' conformation, we rely on the 'solvated' Ramachandran plots shown in Fig. 1B–D. In this respect, alanine is a representative of all residues other than proline and glycine. While it is clear that the conformational energies shown in Fig. 1 are only approximate, they should be accurate enough to allow a rough estimate to be

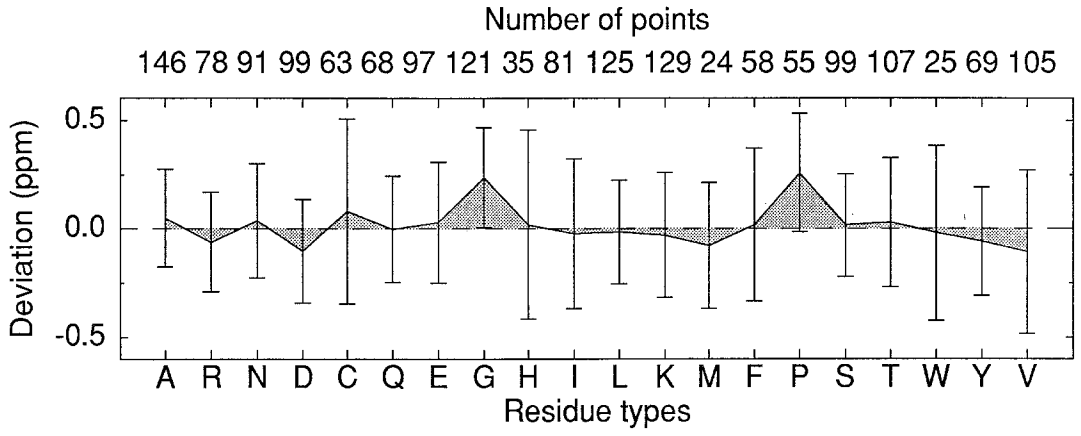

Fig. 2. Mean errors with standard deviations (error bars) for calculated α-proton structural shifts in a database containing 17 proteins (Ösapay and Case, 1991). Distribution of deviations from experimental values and number of data points are shown by residue type.

made of the 'random coil' shifts that arise from a Boltzmann average over this surface. These results are reported in Table 2. The computed peptide contribution to δ_{const} is smaller for proline and glycine than for alanine. This might have been expected just from a visual examination of Fig. 1: the regions near $\phi = -120$ (where the contribution to δ_{const} is largest) are less important for glycine and proline than for alanine. This is especially true for glycine, where large regions of positive ϕ are available to the unstructured peptide. The table indicates that there is not much difference in these averages between the vacuum and MEAD-solvated potential, suggesting that the details of the potential surface are not crucial to the argument.

This general difference between proline/glycine and other amino acids was evident in our earlier empirical study of proton chemical shifts (Ösapay and Case, 1991). In that study, we used a constant 'random coil' contribution for all H^{α} protons, equal to 0.75 ppm. Figure 2 shows the average errors between calculated and observed H^{α} shifts as a function of residue type. It is clear that there are significant systematic errors for glycine and proline, but not for other residues. A refit of the data, allowing separate constants for proline and glycine, results in the empirical values shown in Table 2. There is a good agreement between the empirical and calculated values for alanine and glycine, and a less good agreement for proline. It is possible that there are

TABLE 2
BOLTZMANN-AVERAGED H^{α} PEPTIDE CONTRIBUTIONS (ppm) FOR THE Ala, Gly, AND Pro DIPEPTIDES AND EMPIRICAL VALUES FOR δ_{const}

	CHARMm22		Empirically fitted
	Vacuum	MEAD solvent	
Ala	0.75	0.83	0.75
Gly	0.54	0.55	0.51
Pro	0.71	0.70	0.51

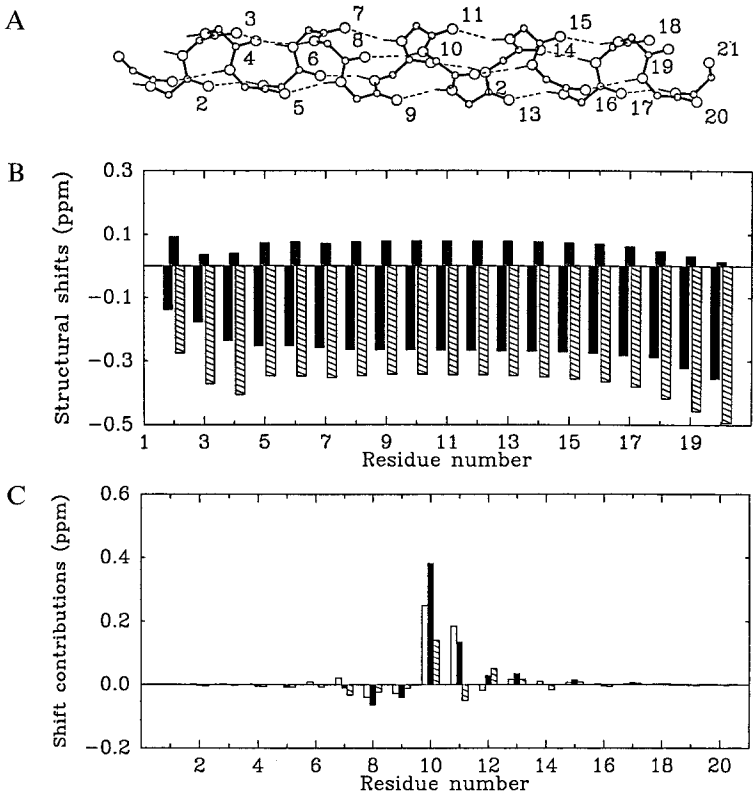

Fig. 3. (A) Model of an α-helix. (B) Structural shifts calculated for α-protons (black bars), alanine β-protons (grey bars), and glycine α3-protons (hatched bars) in the α-helix model. (C) Anisotropy (white bars), electrostatic (hatched bars), and sum of anisotropy and electrostatic contributions (black bars) of peptide groups to chemical shifts for the α-proton of residue 11.

additional restraints, operating in even short proline-containing peptides, that are not included in the simple calculations reported here.

The use of separate constants for proline and glycine can result in significant improvements in predictions for H^{α} shifts in proteins. For example, for 55 proline H^{α} protons included in our earlier database, the rms deviation decreases from 0.371 to 0.237 ppm when the new constant is used. For 121 glycine shifts in the same proteins, the rms error decreases from 0.29 to 0.16 ppm.

Chemical shifts in α-helices

In order to understand the contributions of peptide groups other than the nearest neighbors, we now examine chemical shifts in larger oligopeptide models. Calculated structural shifts in a 21-residue α-helical oligopeptide model are shown in Fig. 3. The solid bars represent the H^{α} proton for L-amino acids, and the hatched bars for D-amino acids (or the $H^{\alpha 2}$ and $H^{\alpha 3}$ positions in glycine, respectively). These are all upfield, with the shifts at the $H^{\alpha 3}$ position being slightly larger. The grey bars show computed shifts at the H^{β} position, which are downfield and considerably smaller. In the middle of the helix the relative environment of each H^{α} proton is nearly the same, and the average computed structural shift is −0.31 ppm. Near the beginning of the helix,

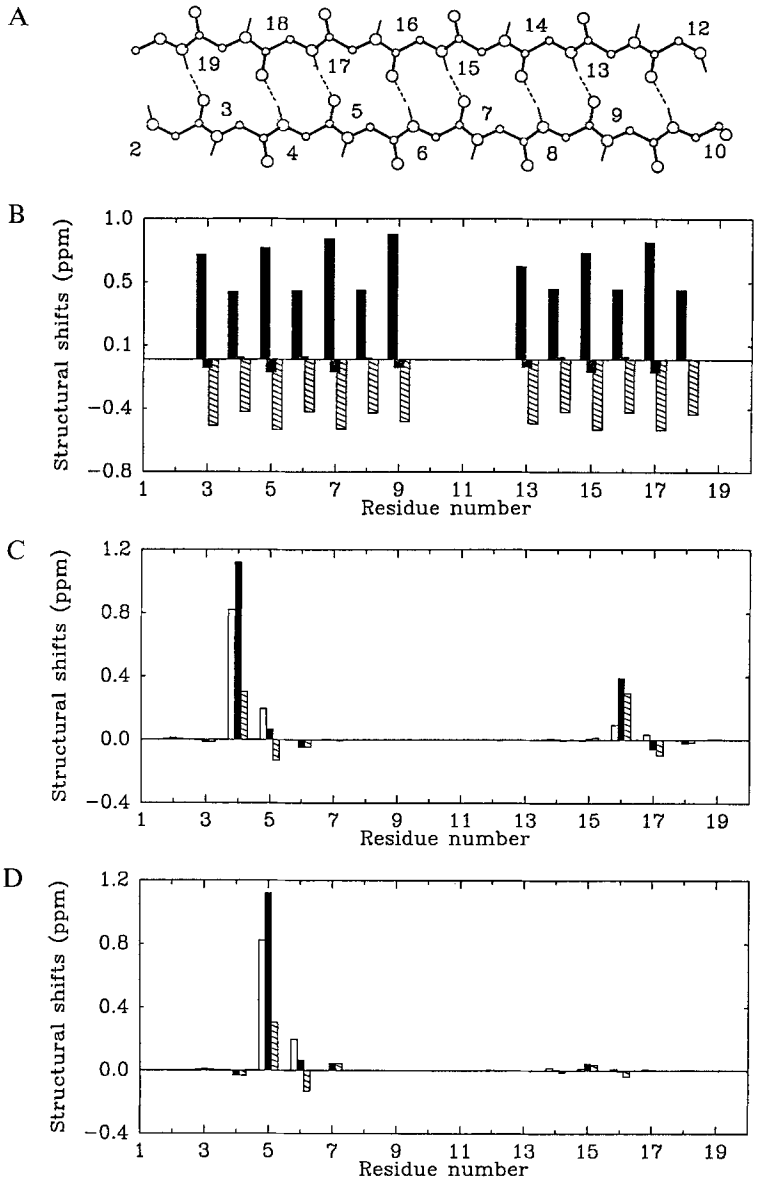

Fig. 4. (A) Model of a two-strand antiparallel β-sheet. (B) Structural shifts calculated for α-protons (black bars), alanine β-protons (grey bars), and glycine α3-protons (hatched bars) in the antiparallel β-sheet model. (C) Anisotropy (white bars), electrostatic (hatched bars), and sum of anisotropy and electrostatic contributions (black bars) to α-proton shift in residue 5. (D) Same as (C) for residue 6.

where there are fewer preceding residues, the shift is less negative, whereas the structural shift is a bit more negative near the C-terminal end of the helix.

These trends are examined in more detail in Fig. 3C, which shows the individual peptide group contributions to the shift of one of the α-protons in the middle of the helix. (The net structural shift is the sum of these contributions minus the 'random coil' constant of 0.75 ppm.) The largest

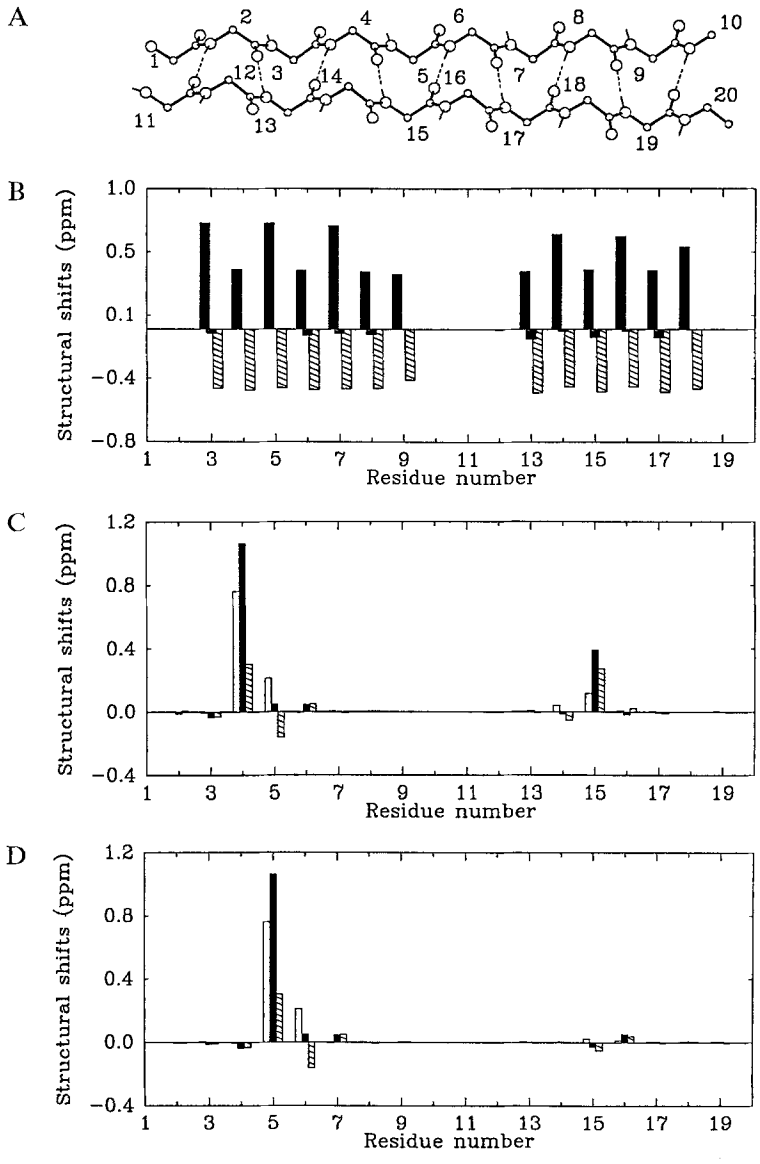

Fig. 5. (A) Same as Fig. 4, for a two-strand parallel β-sheet. Parts (C) and (D) show contributions to the H^{α} shift at positions 5 and 4, respectively.

contribution is from the preceding peptide group, which is consistent with the predominance of the ϕ-angle in modulating shifts, as noted above. The next largest contribution is from the succeeding peptide group, and there are smaller positive contributions arising from the i + 1 and i + 2 positions, and smaller negative contributions from peptide groups i − 2 and i − 3. The change in these smaller contributions explains the trends seen at the N- and C-termini noted above, i.e., there are fewer negative contributions at the N-terminus and fewer positive ones at the C-terminus. In all cases, however, the greatest contributions come from the neighbor peptide

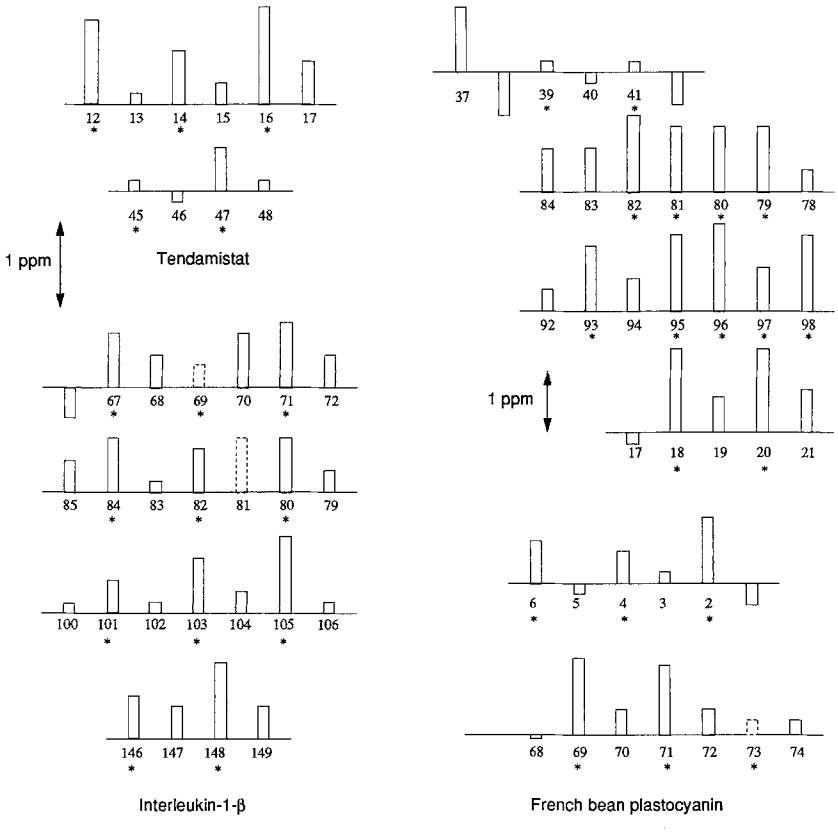

Fig. 6. Experimental structural shifts (corrected by calculated ring-current shifts) for β-strands at the edge of a β-sheet in tendamistat, interleukin 1β and plastocyanin. Residues marked with an asterisk should have significant (positive) shift contributions from peptide groups in an adjacent strand.

groups, where electrostatic contributions are smaller in absolute value than anisotropy contributions, but both contribute to the final results.

Chemical shifts in extended β-chains and sheets

Similar results for a model of two antiparallel β-strands are shown in Fig. 4. Here the net structural shifts at the $H^{\alpha 2}$ position are all positive (downfield), while those at the $H^{\alpha 3}$ position are upfield; structural shifts at the β-position are negative but much smaller. The net structural shift at the $H^{\alpha 2}$ position in a single extended strand is +0.46 ppm, but there is a clear two-residue periodicity in the two-strand results, with shifts alternating between about 0.45 and 0.75 ppm (Fig. 4B). This can be understood by reference to Figs. 4C and D, which show the individual peptide contributions to the shift at the H^{α} position in residues 5 and 6. As can be seen in Fig. 4A, the C^{α} position in residue 5 points 'in' towards the opposite sheet, whereas that in residue 6 is 'out', away from peptide groups on the opposite strand. In each case, the most significant contribution arises from the preceding peptide group, as discussed above; contributions from the succeeding group are quite small in this case, since the anisotropy and electrostatic contributions nearly cancel. For residue 5, though, the electrostatic contribution from the peptide group in the

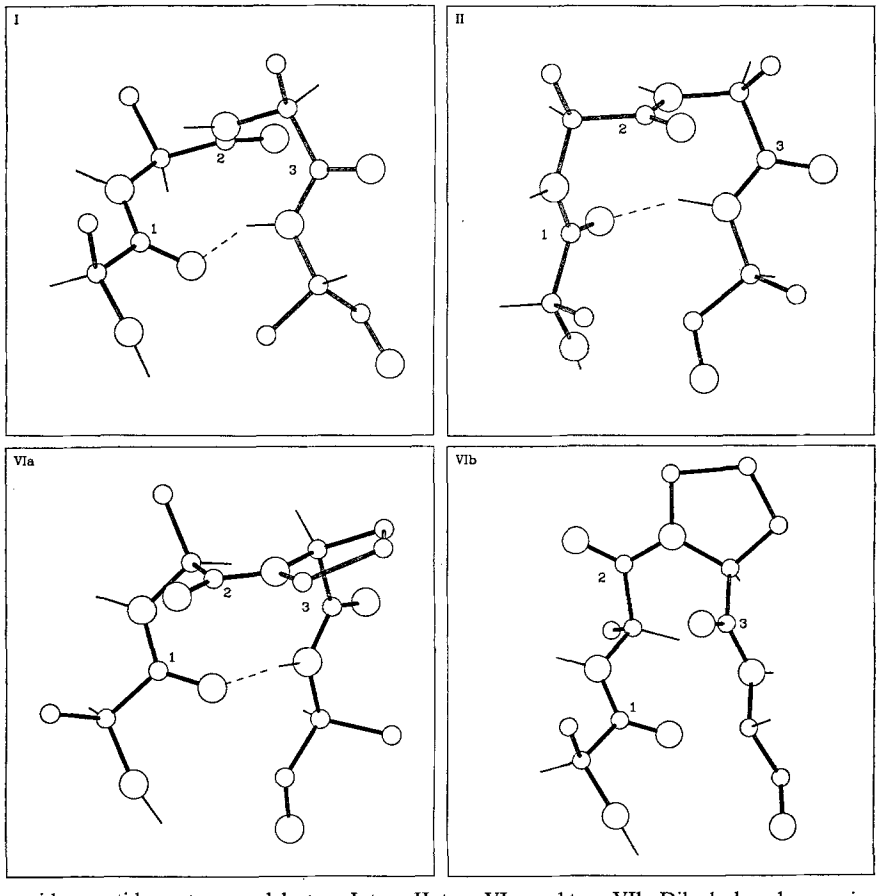

Fig. 7. Four-residue peptides as turn models: turn I, turn II, turn VIa, and turn VIb. Dihedral angles are given in Table 1.

opposite strand makes a significant, positive contribution of about 0.3 ppm, and this contribution is necessarily much weaker at position 6. Since the C^{α} positions along the strand alternate between 'in' and 'out' geometries, this change should lead to twofold periodicity in the shifts at the end of the strands, and we give a variety of examples below where this is observed. Of course, real strands are rarely found in such idealized conformations, but the general rule that cross-strand shift contributions should occur at alternate residues should be a general one.

Similar alternating shifts are observed in a model for a parallel two-stranded β-sheet (Fig. 5). The α-protons in residues that point towards the opposite strand show more positive structural shifts than those in residues pointing away, and the general magnitude of this effect is about the same in these simple models for parallel and antiparallel interactions.

Figure 6 shows examples of this sort of periodicity in regions of β-sheet in tendamistat, plastocyanin and interleukin 1β. In each case, we have plotted the observed H^{α} structural shift, corrected for the (usually small) ring-current contributions that would be predicted from the X-ray crystal structure. Residues marked with an asterisk are in a position to have a significant shift contribution from a neighboring strand, whereas the unmarked residues should have no such shift.

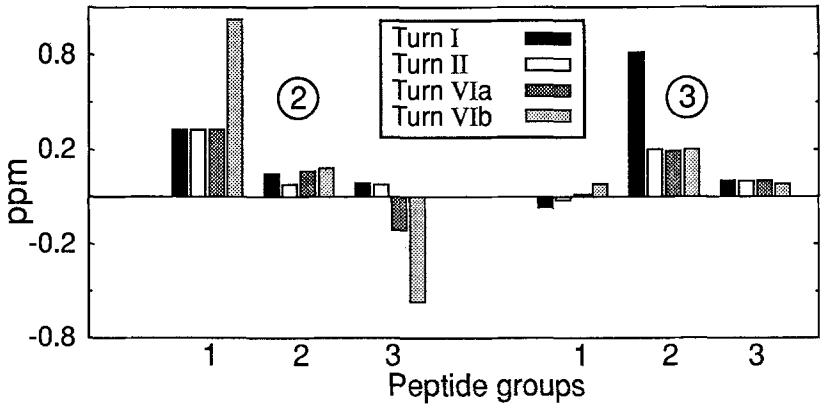

Fig. 8. Peptide-group contributions (sum of anisotropy and electrostatic contributions) to the second (left-hand side) and third (right-hand side) α-protons calculated in the turn models.

In tendamistat (Kline and Wüthrich, 1986), there are two β-strands that have one neighboring antiparallel strand (Pflugrath et al., 1986). The experimental shifts (corrected for the ring-current effects) show clear evidence for twofold periodicity in strands 12–17 and 45–48. The second example is French bean Cu(I) plastocyanin, which consists primarily of two four-stranded β-sheets (Chazin and Wright, 1988; Moore et al., 1991). (Here the ring-current corrections were derived from a model based on the crystal structure of the highly homologous poplar protein (Guss et al., 1986).) The regions 1–6, 17–21, 37–42 and 68–74 at the edges of the sheets clearly show alternating α-proton structural shifts. In the strands in the middle of the sheets (78–84 and

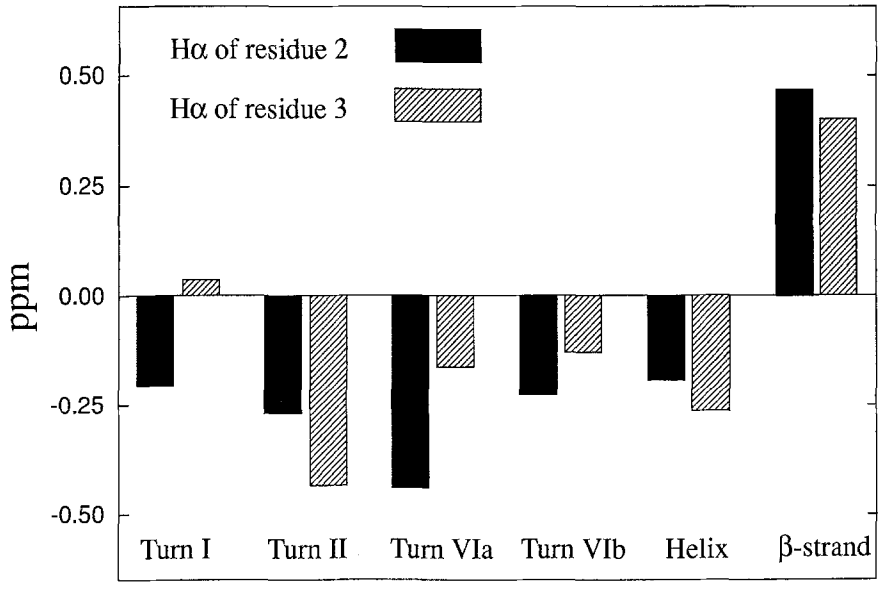

Fig. 9. Net structural shifts for various structures in four-residue peptide models.

92–98) there can often be contributions from both sides, so that the shifts (and the asterisks) do not show the simple two-residue periodicity. Finally, we consider shifts for interleukin 1β, which has a large number of residues in the β-conformation. There are three X-ray structures (Finzel et al., 1989; Priestle et al., 1989; Veerapandian et al., 1992) and we have selected 1I1B (Finzel et al., 1989) for calculating the ring-current corrections. As shown in Fig. 6, in regions 66–72, 79–85, 100–106 and 146–149, the observed shifts show a periodicity that matches their hydrogen-bonding structure: residues involved in cross-strand contacts have a more positive H^{α} proton shift than residues having no interactions with the neighbor strand.

The correlations described above are not universal, even in a qualitative sense, and Fig. 6 shows three examples (in dotted boxes) where the expected relations do not hold. For residue 69 of interleukin 1β, the local structure is not really in the extended region (φ for this residue is −74° in the X-ray structure), so the shift is upfield from what might be expected. Reasons for the other two discrepant shifts (residue 73 in plastocyanin and residue 81 in interleukin 1β) are less clear, and represent either limitations of this analysis or differences between the solution and crystal structures. Nevertheless, the general pattern of twofold periodicity in these three examples suggests that the calculations shown in Figs. 4 and 5 are capturing a real portion of the observed chemical shift dispersion along the protein backbone.

H^{α} chemical shifts in turns

Although there are a great many types of reverse turns in proteins, we focus here on models for four simple idealized structures that characterize types I, II, VIa and VIb (Richardson, 1981). The structures are illustrated in Fig. 7, and torsion angles are given in Table 1. Note that at its core,

TABLE 3
EXPERIMENTAL H^{α} STRUCTURAL SHIFTS IN TYPE I TURNS[a]

Protein	Position 2		Position 3	
Hen egg white lysozyme	Thr^{40}	−0.37	Gln^{41}	0.00
Ribonuclease T1	Gln^{82}	−0.43	Asn^{83}	0.17
Ribonuclease A	Ser^{23}	−0.07	Asn^{24}	0.22
Barley serine proteinase inhibitor	Lys^{72}	−0.16	Leu^{73}	0.05
Tendamistat	Trp^{18}	−0.12	Arg^{19}	0.23
Reduced cytochrome b5	Thr^{33}	−0.80	Lys^{34}	−0.09
	Asp^{82}	−0.34	Asp^{83}	0.18
Bacteriophage T4 lysozyme	Thr^{21}	−0.35	Gln^{22}	0.04
Human ubiquitin	Leu^{8}	−0.17[b]	Thr^{9}	0.01[b]
		−0.09[c]		0.05[c]
	Asp^{39}	−0.41[b]	Glu^{40}	0.11[b]
		−0.33[c]		0.16[c]
Human lysozyme	Thr^{40}	−0.33	Arg^{41}	0.05
	Ile^{56}	−0.01	Phe^{57}	−0.10

[a] Chemical shifts and crystal structures are taken from a database (Ösapay and Case, 1991). Observed shifts have been corrected by the computed ring-current contribution.
[b] Chemical shifts from DiStefano and Wand (1987).
[c] Chemical shifts from Weber et al. (1987).

a turn is characterized by two sets of ϕ, ψ-angles (labeled ϕ_2, ψ_2 and ϕ_3, ψ_3 in Table 1), which fix the positions of *three* peptide groups (labeled 1, 2 and 3 in Figs. 7 and 8).

Figure 8 summarizes the peptide-group contributions to the second and third α-protons in our turn models. Although most of the peptide-group contributions to δ are positive, they are in general less positive than the corresponding contributions in the random-coil state, so that $\Delta\delta$ is generally negative, as shown in Fig. 9. An exception is the shift at position 3 of a type I turn, which is expected to be very slightly downfield from the random-coil position, whereas all other shifts in turns are expected to be shifted upfield. The origin of this downfield bias at position 3 of a type I turn arises primarily from the contribution of the preceding peptide group, which is closer to the maximum downfield shift (at $\phi = -120°$) than are the corresponding residues in the other turns. Similarly, the large positive contribution to H^{α} at position 2 of the type VIb turn is clearly related to its ϕ value of $-140°$. Table 3 presents some examples of observed H^{α} shifts in type I turns in proteins, illustrating the common theme that the shift at position 3 is downfield from that at position 2.

DISCUSSION AND CONCLUSIONS

The calculated net structural shifts for turns, sheets and extended strands are shown in Fig. 9. These illustrate the general expectation of upfield shifts for helices and turns, and downfield shifts for strands and sheets. These results, along with the expected variations within sheets and helices shown in Figs. 3–5, constitute the main results of this paper. The predicted results are in good general agreement with known trends in peptides and proteins, and suggest other regularities that have been less commonly noted.

It is worth remembering that these calculations are based on an empirical model for peptide-group contributions. In real situations, there may be additional shift contributions (e.g. from ring currents or solvent effects) that are not considered here, and even the peptide contribution may not be faithfully represented by such simple formulas. Furthermore, elements of secondary structure in real proteins or peptides will generally deviate from the idealized geometries considered here. Nevertheless, simple calculations on idealized systems provide a real service in suggesting new ways to use chemical shift data in structural terms. For example, there is increasing interest in analyzing shift differences in similar systems to identify the extent of structural similarity, or to locate changes upon ligand binding or other perturbations. Among many examples that might be cited would be analyses of shift changes upon formation of a ternary complex in staphylococcal nuclease (Wang et al., 1992), the binding of calcium to calbindin D_{9k} (Skelton et al., 1992), an analysis of secondary structure in mutant zinc-fingers (Lee et al., 1992), a comparison of shifts in interleukin analogues (Stockman et al., 1992), and an analysis of the interaction between proteins in a bacterial phosphotransferase system (Chen et al., 1993). Similar comparisons are also useful for linear peptides, where the (general) extent of conformational heterogeneity hampers quantitative NOE-based structure calculations. For example, amide proton shifts in model helical peptides are often periodic (with a 3–4 residue repeat pattern) (Kuntz et al., 1991; Jiménez et al., 1992); amphipathic helices show a periodic behavior that appears to be related to curving of the helix axis (Blanco et al., 1992; Zhou et al., 1992); and it may be possible to characterize helices of marginal stability through an analysis of the solvent dependence of backbone shifts (Bruix et al., 1990). The calculations reported here should be useful in further comparisons of this kind.

ACKNOWLEDGEMENTS

We thank Don Bashford, Rafael Brüschweiler and Peter Wright for helpful discussions. This work was supported by NIH grant GM-45811.

REFERENCES

Andersen, N.H., Cao, B. and Chen, C. (1992) *Biochem. Biophys. Res. Commun.*, **184**, 1008–1014.
Anderson, A.G. and Hermans, J. (1988) *Protein Struct. Funct. Genet.*, **3**, 262–265.
Asakura, T., Niizawa, Y. and Williamson, M.P. (1992) *J. Magn. Reson.*, **98**, 646–653.
Bashford, D., Case, D.A., Dalvit, C., Tennant, L. and Wright, P.E. (1993) *Biochemistry*, **32**, 8045–8056.
Bashford, D. and Gerwert, K. (1992) *J. Mol. Biol.*, **224**, 473–486.
Bashford, D. and Karplus, M. (1990) *Biochemistry*, **29**, 10219–10225.
Blanco, F.J., Herranz, J., González, C., Jiménez, M.A., Rico, M., Santoro, J. and Nieto, J.L. (1992) *J. Am. Chem. Soc.*, **114**, 9676–9677.
Bondi, A. (1964) *J. Chem. Phys.*, **40**, 441–451.
Brooks, B.R., Bruccoleri, R.E., Olafson, B.D., States, D.J., Swaminathan, S. and Karplus, M. (1983) *J. Comput. Chem.*, **4**, 187–217.
Brooks III, C.L. and Case, D.A. (1993) Chem. Rev., **93**, 2487–2502.
Bruix, M., Perello, M., Herranz, J., Rico, M. and Nieto, M.L. (1990) *Biochem. Biophys. Res. Commun.*, **167**, 1009–1014.
Buckingham, A.D. (1960) *Can. J. Chem.*, **38**, 300–307.
Bundi, A. and Wüthrich, K. (1979) *Biopolymers*, **18**, 285–297.
Chazin, W.J. and Wright, P.E. (1988) *J. Mol. Biol.*, **202**, 623–636.
Chen, Y., Reizer, J., Saier Jr., M.H., Fairbrother, W.J. and Wright, P.E. (1993) *Biochemistry*, **32**, 32–37.
Cross, K.J. and Wright, P.E. (1985) *J. Magn. Reson.*, **64**, 220–231.
Dalgarno, D.C., Levine, B.A. and Williams, R.J.P. (1983) *Biosci. Rep.*, **3**, 443–452.
De Dios, A.C., Pearson, J.G. and Oldfield, E. (1993) *Science,* **260**, 1491–1496.
Distefano, D.L. and Wand, A.J. (1987) *Biochemistry*, **26**, 7272–7281.
Finzel, B.C., Clancy, L.L., Holland, D.R., Muchmore, S.W., Watenpaugh, K.D. and Einspahr, H.M. (1989) *J. Mol. Biol.*, **209**, 779–791.
Grant, J.A., Williams, R.L. and Scheraga, H.A. (1990) *Biopolymers*, **30**, 929–949.
Guss, J.M., Harrowell, P.R., Murata, M., Norris, V.A. and Freeman, H.C. (1986) *J. Mol. Biol.*, **192**, 361–387.
Haigh, C.W. and Mallion, R.B. (1980) *Prog. NMR Spectrosc.*, **13**, 303–344.
Harris, R.K. (1986) *Nuclear Magnetic Resonance Spectroscopy - A Physicochemical View*, Longman, Harlow.
Honig, B., Sharp, K. and Yang, A.-S. (1993) *J. Phys. Chem.*, **97**, 1101–1109.
Jiménez, M.A., Blanco, F.J., Rico, M., Santoro, J., Herranz, J. and Nieto, J.L. (1992) *Eur. J. Biochem.*, **207**, 39–49.
Kline, A.D. and Wüthrich, K. (1986) *J. Mol. Biol.*, **192**, 869–890.
Kuntz, I.D., Kosen, P.A. and Craig, E.C. (1991) *J. Am. Chem. Soc.*, **113**, 1406–1408.
Lee, M.S., Palmer III, A.G. and Wright, P.E. (1992) *J. Biomol. NMR*, **2**, 307–322.
McConnell, H.M. (1957) *J. Chem. Phys.*, **27**, 226–229.
Moore, J.M., Lepre, C., Gippert, G.P., Chazin, W.J., Case, D.A. and Wright, P.E. (1991) *J. Mol. Biol.*, **221**, 533–555.
Ösapay, K. and Case, D.A. (1991) *J. Am. Chem. Soc.*, **113**, 9436–9444.
Ösapay, K., Case, D.A. and Cross, K.J. (1991) *SHIFTS Program*, The Scripps Research Institute, La Jolla, CA.
Pardi, A., Wagner, G. and Wüthrich, K. (1983) *Eur. J. Biochem.*, **137**, 445–454.
Pastore, A. and Saudek, V. (1990) *J. Magn. Reson.*, **90**, 165–176.
Pearlman, D.A., Case, D.A., Caldwell, J.C., Seibel, G.L., Singh, U.C., Weiner, P. and Kollman, P.A. (1991) *AMBER 4.0*, University of California, San Francisco, CA.
Pettitt, M. and Karplus, M. (1988) *J. Phys. Chem.*, **92**, 3994–3997.
Pflugrath, J.W., Wiegand, G., Huber, R. and Vertesy, L. (1986) *J. Mol. Biol.*, **189**, 383–386.
Priestle, J.P., Shaer, H.-P. and Gruetter, M.G. (1989) *Proc. Natl. Acad. Sci. USA*, **86**, 9667–9671.
Richardson, J.S. (1981) *Adv. Protein Chem.*, **34**, 167–339.

Sharp, K.A. and Honig, B. (1990) *Annu. Rev. Biophys. Biophys. Chem.*, **19**, 301–332.
Skelton, N.J., Akke, M., Kördel, J., Thulin, E., Forsén, S. and Chazin, W.J. (1992) *FEBS Lett.*, **303**, 136–140.
Spera, S. and Bax, A. (1991) *J. Am. Chem. Soc.*, **113**, 5490–5492.
Stockman, B.J., Scahill, T.A., Strakalaitis, N.A., Brunner, D.P., Yem, A.W. and Deibel Jr., M.R. (1992) *J. Biomol. NMR*, **2**, 591–596.
Szilágyi, L. and Jardetzky, O. (1989) *J. Magn. Reson.*, **83**, 441–449.
Veerapandian, B., Gilliland, G.L., Raag, R., Svensson, A.L., Masui, Y., Hirai, Y. and Poulos, T.L. (1992) *Protein Struct. Funct. Genet.*, **12**, 10–23.
Wang, J., Hinck, A.P., Loh, S.N., LeMaster, D.M. and Markley, J.L. (1992) *Biochemistry*, **31**, 921–936.
Warshel, A. and Aqvist, J. (1991) *Annu. Rev. Biophys. Biophys. Chem.*, **20**, 267–298.
Weber, P.L., Brown, S.C. and Mueller, L. (1987) *Biochemistry*, **26**, 7282–7290.
Williamson, M.P. (1990) *Biopolymers*, **29**, 1423–1431.
Williamson, M.P. and Asakura, T. (1991) *J. Magn. Reson.*, **94**, 557–562.
Williamson, M.P. and Asakura, T. (1993) *J. Magn. Reson. Ser. B*, **101**, 63–71.
Williamson, M.P., Asakura, T., Nakamura, E. and Demura, M. (1992) *J. Biomol. NMR*, **2**, 83–98.
Wishart, D.S., Sykes, B.D. and Richards, F.M. (1991) *J. Mol. Biol.*, **222**, 311–333.
Wishart, D.S., Sykes, B.D. and Richards, F.M. (1992) *Biochemistry*, **31**, 1647–1651.
Zhou, N.E., Zhu, B.-Y., Sykes, B.D. and Hodges, R.S. (1992) *J. Am. Chem. Soc.*, **114**, 4320–4326.